International Journal of Applied Mathematics and Theoretical Physics
2022; 8(2): 30-42
http://www.sciencepublishinggroup.com/j/ijamtp
doi: 10.11648/j.ijamtp.20220802.11
ISSN: 2575-5919 (Print); ISSN: 2575-5927 (Online)

Thermophoresis and Viscous Dissipation Effect of Free Convective Boundary Layer Flow over a Porous Medium: Spectral Homotopy Analysis

Chika Uchechukwu Boneze[1], Adeolu John Omowaye[2], Adeyemi Isaiah Fagbade[2], Ayodele Adedeji Ashefon[1]

[1]Department of Mathematics, University of Louisiana, Lafayette, U.S.A
[2]Department of Mathematical Sciences, Federal University of Technology, Akure, Nigeria

Email address:
bonezechika@gmail.com (Chika Uchechukwu Boneze)

To cite this article:
Chika Uchechukwu Boneze, Adeolu John Omowaye, Adeyemi Isaiah Fagbade, Ayodele Adedeji Ashefon. Thermophoresis and Viscous Dissipation Effect of Free Convective Boundary Layer Flow over a Porous Medium: Spectral Homotopy Analysis. *International Journal of Applied Mathematics and Theoretical Physics*. Vol. 8, No. 2, 2022, pp. 30-42. doi: 10.11648/j.ijamtp.20220802.11

Received: March 10, 2022; **Accepted**: July 11, 2022; **Published**: August 17, 2022

Abstract: In this study, an investigation is made into the effects of thermophoresis and viscous dissipation on chemically steady hydromagnetic free convective boundary layer flow in a porous media. A mathematical model was designed to govern the flow used in the study of the effects of chemical reaction, magnetic field, viscous dissipation, and thermophoresis on free convective boundary layer flow of an incompressible, electrically conducting fluid past a heated vertical permeable flat plate embedded in a uniform porous medium. This flow is observed as it moves past the plate, which is embedded in a uniform porous medium. The governing equations and their related boundary conditions have been converted into dimensionless equations by using the similarity transformations. These dimensionless equations are a boundary valued problem of coupled ordinary differential equations, and they have been solved by employing the Spectral Homotopy Analysis Method, which is a numerical approach of the traditional Homotopy Approximate Method (HAM). The Chebyshev-Gauss-Lobatto points are used to discretize the spatial domains, and numerical computation is used to determine the non-dimensional properties of the physical parameters. The SHAM solution series converges to the numerical solution with an accuracy of up to six decimal places, as demonstrated by our simulations. A parametric investigation of some of the parameters that are available is carried out, and the results for velocity, temperature, and concentration are graphically displayed, in addition to the discussion of the physical components of the issue. When the computational results from SHAM and those from the literature are compared to one another, they show a good degree of agreement with one another. It has been determined that the flow parameters have a significant impact on the flow profiles, and this connection has been investigated in depth. Findings that are really significant.

Keywords: Thermophoresis, Viscous Dissipation, Porous Medium, Magnetic Effect, Chemical Reaction, Spectral Homotopy Analysis Method (SHAM)

1. Introduction

The phenomenon of thermophoresis, which is often referred to as thermomigration, is seen in mixes of mobile particles and describes how they respond differentially to temperature gradients. Aerosol mixtures including dust, fog, forest exudates, and geyser steam are usually referred to by this word. All phases of matter frequently discuss thermophoresis. There are numerous real-world uses for the thermophoretic force. The major reason for its utilization is that different particles behave differently when a temperature gradient is present. After they have been mixed together, these particle kinds can be separated by that force, or if they have already separated, they can be kept from combining. Since the hotter side of a semiconductor wafer has a more readily available transition that is needed for an atomic leap, impurity ions may travel from the cold side to the hot side of the wafer. Commercial precipitators have utilized thermophoretic force for uses such as electrostatic

precipitators. It is used in vacuum deposition procedures for the production of optical fibers. Thermophoresis has also been demonstrated to offer the ability to speed up drug recovery by enabling the identification of parameter binding through a comparison of the target molecule's motion when bound and unbound. Additionally, it has been shown that thermophoresis provides a flexible method for controlling single biological macromolecules, such as genomic-length DNA and HIV virus, in micro and nano-channels by using light-induced local heating. One technique used in the field flow fractionation to separate various polymer particles is thermophoresis. The magnitude of the thermophoresic force and velocity exhibit proportionality to the temperature gradient. This significantly depends on variables like the carrier gas's and the aerosol particles' thermal conductivity. Kerosene combustion results in the glass of a lantern's glass globe becoming darkened. Simply put, this exemplifies thermophoresis. Due to the temperature differential between the flame and the glass globe, the carbon particles emitted during combustion are drawn towards the glass globe where they eventually rest. Although many researchers have studied thermophoresis, Goren [1] was one of the first to focus on how important it is in laminar flow over a horizontal plate. He took into account both hot and cold plates in this plate. The combined effects of chemical reaction, radiation on heat, and mass transport along a constantly moving surface in the presence of thermophoresis were examined by Chandra and Kumar [2]. Incompressible viscous flow based on magnethydrodynamics (MHD) has many applications in research and engineering, particularly when it comes to heat and mass transfer driven by chemical reaction. It is used in a variety of industries, including crystal growth, agricultural and petroleum industries, and metal extrusion. Foreign matter and the fluid that the plate is travelling through will always undergo chemical reactions in various chemical reactions, and this process has many industrial benefits and applications. Production of glass or ceramics, food processing, and polymer production are a few examples. In chemical kinetics, the index or exponent raised by the concentration term of a specific substance in the rate equation is used to describe the order of reaction with regard to that substance (such as reactant, catalyst, or product). In other words, an order n reaction is one whose reaction rate is n-power proportional to the concentration. A first-order reaction is specifically one in which the pace of the reaction is precisely proportional to the concentration of the reacting component. Any chemical reaction that takes place in a single phase is referred to as a homogeneous reaction (gaseous, liquid, or solid). Since the nature of interactions between the reacting substances determines the only chemical changes that occur, homogeneous reactions are simpler theoretically. Any chemical reaction in which the reactants are components of two or more phases (solid and gas, solid and liquid, or two immiscible liquids), or in which one or more reactants undergo chemical changes at an interface, is referred to as a heterogeneous reaction.

Heterogeneous reactions include the reactions of metals with acids, the electrochemical alterations that take place in batteries and electrolytic cells, and the process of corrosion. According to Alam et al. [3], a reaction that persists at an interface is heterogeneous, but a reaction that persists in a solution is heterogeneous.

A few researchers and their works will be examined, however many have investigated chemical reactions. The effects of mass transfer on the flow through an infinite, vertical plate that was started abruptly and had constant heat flux and chemical reaction were examined by Das et al. [4]. Anjah and Kandasamy investigated the impact of chemical reaction MHD flow with heat and mass transmission past a semi-infinite plate [5]. In the presence of a heat source and the thermal stratification effect, Kandasamy et al. [6] investigated the impact of chemical reaction on MHD flow with heat and mass transfer over a vertically stretched sheet. Odat and Al-Azab conducted a study on the impact of chemical reactions on transient MHD free convection over a moving vertical plate [7]. Ahmed [8] examined how chemical reactions affected transient MHD free convective flow over a vertical plate in the slip flow regime. A study on mass transfer with chemical reaction on hydromagnetic flow and heat transfer on a constantly moving surface was conducted by Jat and Chandry [9].

Viscous heating is the result of an irreversible process in which heat is produced as a result of work being done by a fluid on neighboring layers as a result of the action of shear force. The link between the energy and momentum equations makes viscous heating very advantageous for fluids with large temperature-dependent viscosities. The rate at which mechanical energy is transformed into thermal energy in a viscous fluid per unit volume is known as viscous heating, especially in porous media. Despite the viscous dissipation's critical role in the natural convective flow, few few academics have studied its impacts over the years. Gebhart [10] looked at the significance of viscous dissipative heat in free convection flow in the condition of isothermal and constant heat flux in the plate to demonstrate its significance. Takhar and Beg [11] provided a model of viscous dissipation in a porous medium past a vertical porous plate. Murthy and Sing [12] investigated the impact of viscous dissipation in relation to incompressible fluid in a saturated porous material. Rees et al [13]'s investigation of the influence of viscous dissipation on boundary layer flow formation from a cold vertical surface immersed in a porous Darcian medium. Nield [14] talked about viscous dissipation in a saturated porous media and its applicability to either forced convection or natural convection. He discussed the significance of its application in some porous media, such as food storage, heat removal from nuclear fuel debris, exothermic and/or endothermic chemical processes, dissociating fluid in packed-bed reactors, and underground disposal of radioactive wastes. According to Loganathan and Arasu [15], there are further benefits to utilizing desposition mechanisms for greater efficiency when applying pigments, metal coatings, or gas stream filtering. Radioactive particles that are deposited as a result of thermophoresic activity are acknowledged to occur in nuclear reactor accidents. Sulfur and

nitrogen oxides that are released into the atmosphere will combine with water molecules to generate acids, which will then fall as acid rain. Mahdy [16] investigated the effects of changing viscosity and the deposition of thermophoresic particles on Non-Darcy free convection in a fluid saturated with uniform suction on injection.

A boundary layer flow across a porous wedge was examined by Felix Ilesanmi Alao et al. [17] for the effects of heat radiation, soret, and dufour in the presence of suction or injection. Muhaimin et al. [18] looked studied the combined effects of thermophoresis and chemical reaction on non-Darcy MHD mixed convective heat and mass transfer across a porous wedge when suction or injection is present. Kishan and Maripala [19] thought about the impact of viscous dissipation and thermophoresis on Darcy-Forcheimer MHD mixed convection in a fluid-saturated porous medium. Fagbade et al. [20] demonstrated how the magnetic field, viscous dissipation, and thermophoresis affect Darcy-Forcheimer mixed convection flow in a fluid-saturated porous material. According to all of these studies, no one has looked into or analyzed the impact of thermophoresis and viscous dissipation effects on chemically steady hydromagnetic free convective boundary layer flow in a porous media. the study will therefore be conducted utilizing the Spectral Homotopy Analytical Method (SHAM).

2. Problem Formulation in Mathematics

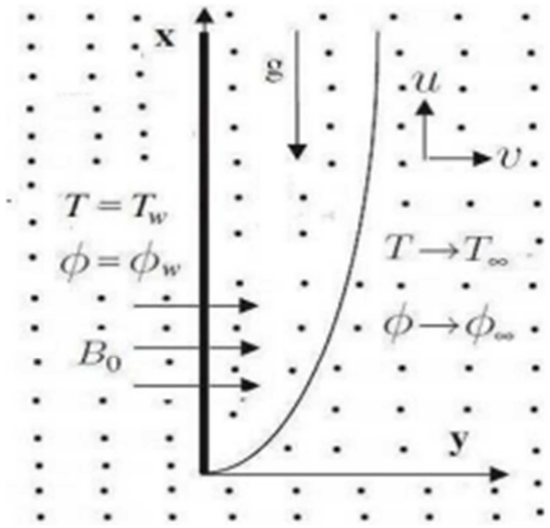

Figure 1. *Physical geometry of the model.*

Take into account a fluid flowing in a steady, laminar, hydromagnetic free convective boundary layer on a porous medium while also experiencing thermophoresis and the viscous dissipation effect. The y-coordinate is normal to the leading edge of the medium, and the x-coordinate is measured along that edge. A first order homogeneous chemical reaction is presummated to occur in the flow, and the fluid characteristics are assumed to be constant. The porous medium is thought to be uniformly distributed and in local thermodynamic equilibrium. It should be noted that the porous plate's hole size is taken to be constant. Understanding the change in mass deposition on the surface requires an understanding of the chemical reaction occurring in the flow and the impact of thermophoresis.

The governing boundary layer equations for this inquiry, which are based on the balancing laws of mass, linear momentum, energy, and concentration species, can be expressed as follows under these assumptions and the Boussinesq approximation:

$$\frac{\partial u}{\partial x} + \frac{\partial v}{\partial y} = 0 \tag{1}$$

$$u\frac{\partial u}{\partial x} + v\frac{\partial v}{\partial y} = \vartheta\frac{\partial^2 u}{\partial y^2} - u\frac{\sigma {\beta_0}^2}{\rho} + g\beta_T(T - T_\infty) + g\beta_C(C - C_\infty) - \frac{\vartheta}{K}u \tag{2}$$

$$u\frac{\partial T}{\partial x} + v\frac{\partial T}{\partial y} = \propto \frac{\partial^2 T}{\partial y^2} + \frac{\mu\sigma {\beta_0}^2}{\rho C_p}\left(\frac{\partial u}{\partial y}\right)^2 \tag{3}$$

$$u\frac{\partial C}{\partial x} + v\frac{\partial C}{\partial y} = D_m\frac{\partial^2 C}{\partial y^2} - \frac{\partial}{\partial y}V_T(C - C_\infty) \tag{4}$$

depending on the starting circumstances.

$$u = Bx,\ v = V,\ C = Cw = C\infty + bx,\ T = Tw = T\infty + ax$$

$$at\ y \to 0 \tag{5}$$

And the boundary conditions are:

$$u \to 0, C \to C\infty, T \to T\infty\ as\ y \to \infty \tag{6}$$

The gradient of ambient temperature and concentration profiles stratifies at a rate of a and b, where b is a constant.

While the components of velocity in the x and y directions, respectively, are u and v.

Following Talbot et al. [21], the term in equation (4) is defined as:

$$V_T = -k\nu\frac{\nabla T}{Tref} = -k\nu\frac{\partial T}{\partial y} \tag{7}$$

Assuming the relations that follow:

$$u = \frac{\partial\psi}{\partial y};\ v = -\frac{\partial\psi}{\partial x};\ \theta(\eta) = \frac{T - T\infty}{Tw - T\infty};\ \phi(\eta) = \frac{C - C\infty}{Cw - C\infty} \tag{8}$$

It is well known that boundary layer flows have a predominant flow direction and boundary layer thickness is small compared to a typical length in the main flow direction.

We introduce the following non-dimensional variables:

$$\eta = y\sqrt{\frac{B}{v}};\ \psi = x\sqrt{Bv}\,f(\eta);$$

$$C = C\infty + (Cw - C\infty)\phi(\eta);\ T = T\infty + (Tw - T\infty)(\eta) \tag{9}$$

The stream function in this case is (x, y).

The equation for continuity is satisfied by the mathematical relations (8) and (9) (1).

The following nondimensional equations are produced by substituting the aforementioned transformations into the

governing equations (1) through (4):

$$f'''+ff''-(f')^2+Gr\theta+Gm\phi-(M+\lambda f')=0 \quad (10)$$

$$\theta''+Prf\theta'+PrEc(f'')^2-Prf'\theta=0 \quad (11)$$

$$\phi''+Scf\phi'-\tau Sc(\theta''\phi+\theta'\phi')=0 \quad (12)$$

where the relevant dimensionless flow parameters are specified as: and the prime imply differentiation with respect to

$$M=\frac{\sigma{\beta_0}^2}{\rho}B;\ Pr=\frac{v}{\propto};\ Sc=\frac{v}{D_m};\ Ec=\frac{x^2B^2}{C_p(T_w-T_\infty)}$$

$$\tau=\frac{kB(T_w-T_\infty)}{Tref};\ \lambda=\frac{v}{kB};\ Gr=\frac{g\beta T(T_w-T_\infty)}{xB^2};\ Gm=\frac{g\beta T(C_w-C_\infty)}{xB^2}$$

The modified boundary conditions are as follows:

$$f(0)=-f_w;\ f'(0)=1;\ \theta(0)=1;\ \phi(0)=1 \quad (13)$$

$f_w=\sqrt{\frac{V}{Bv}}$ is the suction velocity without dimensions. It is interesting to observe that when Ec = λ = τ = 0, which simplifies the current issue to the models examined by Gangadhar and Bhaskar [29] and Ibrahim and Makinde [28], respectively.

The following physical quantities are relevant to this issue:

The definitions of skin friction coefficient, Nusselt number, and Sherwood number are as follows:

$$f''(0)=\frac{1}{2}Re_x^{\frac{1}{2}}C_f;\ -\theta'(0)=\frac{1}{2}Re_x^{-\frac{1}{2}}Nu;$$

$$-\phi'(0)=\frac{1}{2}Re_x^{-\frac{1}{2}}Sh;\ Re_x^{\frac{1}{2}}=\sqrt{\frac{U\infty}{\nu}}(Reynolds\ number)$$

3. Method of Solution: SHAM

Because of their elegance and high accuracy in resolving issues with smooth functions, spectral methods are increasingly being used to solve ordinary and partial differential equations Canuto et al. [22] and Trefethen [23]. Motsa [27] transformed the homotopy analysis approach (Liao [23, 24]) into the spectral homotopy analysis method (SHAM). The problem of viscous dissipation and thermophoresis effects on chemically reacting steady hydromagnetic free convective boundary layer flow over a vertical plate in a porous medium was solved using a set of ordinary differential equations (ODEs) in this work. With applications in applied mathematics, physics, nonlinear mechanics, finance, and engineering, it is frequently used to solve many types of nonlinear ordinary and partial differential equations. SHAM is employed in Motsa [25, 26] and Fagbade et al. [19] and combines the Chebyshev spectral collocation approach with the traditional HAM's guiding principles to solve the transformed sequence of ordinary differential equations. The elimination of the need to adhere to a certain rule of solution expression is one of the SHAM's key advantages. Additionally, the SHAM demands that the complete linear component of the governing differential equation be chosen as the linear operator to be employed in the algorithm's development. The Chebyshev spectral collocation method is used since this frequently results in complex series of linear ordinary differential equations that can only be solved numerically. It is customary to first change the problem's domain from [0,∞] to [-1,1] before employing the spectral homotopy analysis method to make the governing boundary conditions homogeneous.

$$\zeta=\frac{2\eta}{L}-1;\ \zeta\in[-1,1]$$

$$f(\eta)=(\zeta)+f_0(\eta);\ (\eta)=(\zeta)+\theta_0(\eta);\ (\eta)=(\zeta)+\phi_0(\eta) \quad (14)$$

$$f_0(\eta)=1-f_w-e^{-\eta};\ \theta_0(\eta)=e^{-\eta};\ \phi_0(\eta)=e^{-\eta} \quad (15)$$

When the governing equation and boundary conditions (10) and (13) are entered into equations (14) and (15), the results are as follows:

$$f'''+ff''+a_1f+a_2f''-(f')^2+Gr\theta+Gm\phi-(M+\lambda)f'=A_1(\eta) \quad (16)$$

$$\theta''+Prf\theta'+b_1Prf+b_2Pr\theta'+PrEc(f'')^2+b_3PrEcf''-Prf'\theta-b_4Prf'+\frac{1}{2}Pra_3\theta=A_2(\eta) \quad (17)$$

$$\phi''+Scf\phi'+c_1Scf+c_2Sc\phi'-Sc\tau\theta''\phi-Sc\tau c_3\theta''-Sc\tau b_5\phi-Sc\tau\theta'\phi'-Sc\tau c_1\theta'$$
$$-Sc\tau b_1\phi'-Scf'\phi-c_3Scf'-a_4Sc\phi=A_3(\eta) \quad (18)$$

Depending on

$$(-1)=f'(1)=0;\ \theta(-1)=\theta(1)=0;\ \phi(-1)=\phi(1)=0 \quad (19)$$

where difference with respect to the primes is indicated.

$$a_1=f_0''(\eta);\ a_2=f_0(\eta);\ a_3=-2f_0'(\eta);\ a_4=f_0'(\eta);\ b_1=\theta_0'(\eta);\ b_2=f_0(\eta);\ b_3=2f_0''(\eta);$$
$$b_4=\theta_0(\eta);\ b_5=\theta_0''(\eta);\ c_1=\phi_0'(\eta);\ c_2=f_0(\eta);\ c_3=\phi_0(\eta) \quad (20)$$

And

$$A_1(\eta) = -f_0'''(\eta) - f_0(\eta)f_0''(\eta) + (f_0'(\eta))^2 - \theta_0(\eta) - G\,\phi_0(\eta) + (M + \lambda)f_0'(\eta) \quad (21)$$

$$A_2(\eta) = -\theta_0''(\eta) - P\,r\,f_0(\eta)\theta_0'(\eta) - P\,r\,E\,c\,(f_0''(\eta))^2 + f_0'(\eta)\theta_0(\eta) \quad (22)$$

$$A_3(\eta) = -\phi_0''(\eta) - S\,c\,f_0(\eta)\phi_0'(\eta) + S\,c\,\tau\,\theta_0''(\eta)\phi_0(\eta) + S\,c\,\tau\,\theta_0'(\eta)\theta_0'(\eta) + S\,c\,f_0'(\eta)\,\phi_0(\eta) \quad (23)$$

The non-homogeneous linear component of the solutions to the governing equations (16) through (18) is regarded as the initial approximation and is denoted as follows:

$$f_l''' + a_1 f_l + a_1 f_l'' + a_3 f_l' + G\,r\,\theta_l + G\,m\,\phi_l - (M + \lambda)f_l' = A_1(\eta) \quad (24)$$

$$\theta_l'' + b_1 P\,r\,f_l + b_2 P\,r\,\theta_l' + b_3 P\,r\,E\,c\,f_l'' - P\,r\,b_4 f_l' + \frac{1}{2}P\,r\,a_3\theta_l = A_2(\eta) \quad (25)$$

$$\phi_l'' + c_1 S\,c\,f_l + c_2 S\,c\,\phi_l' - \tau\,S\,c\,\theta_l'' - \tau\,S\,c\,b_5\phi_l - c_1 S\,c\,\tau\,\theta_l' - S\,c\,\tau\,b_1\phi_l' - c_3 S\,c\,f_l' - a_4 S\,c\,\phi_l = A_3(\eta) \quad (26)$$

Depending on

$$f_l(-1) = f_l'(1) = 0;\ \theta_l(-1) = \theta_l\,(1) = 0\ \phi_l(-1) = \phi_l(1) = 0 \quad (27)$$

To resolve (24) -, we employ the Chebyshev pseudospectral technique (27)

An approximation of the unknown function is given by a truncated series of Chebyshev polynomials of the following form:

$$f_l(\xi) \approx \sum_{k=0}^{Q} \widehat{f_k}\, P_k(\xi_j)\ j\ = 0, 1, \ldots, Q \quad (28)$$

$$\theta_l(\xi) \approx \sum_{k=0}^{Q} \widehat{\theta_k}\, P_k(\xi_j)\ j\ = 0, 1, \ldots, \quad (29)$$

$$\phi_l(\xi) \approx \sum_{k=0}^{Q} \widehat{\phi_k}\, P_k(\xi_j)\ j\ = 0, 1, \ldots, \quad (30)$$

where P_k is the k th Chebyshev polynomial, $\widehat{f_k}$, $\widehat{\theta_k}$ and $\widehat{\phi_k}$ are coefficients and $\xi_0, \xi_1, \ldots, \xi_Q$ are Gauss-Lobatto collocation points (see [21]) defined by

$$\xi_j = \cos\left(\frac{\pi j}{Q}\right);\ j\ = 0, 1, \ldots,$$

Derivatives of the functions $f_l(\xi)$, $\theta_l(\xi)$ and $\phi_l(\xi)$ at the collocation points are represented as

$$\frac{d^r f_l}{\xi^r} = \sum_{k=0}^{Q} D_{kj}^r f_l(\xi_j)\ \frac{d^r \theta_l}{\xi^r} = \sum_{k=0}^{Q} D_{kj}^r \theta_l(\xi_j);\ \frac{d^r \phi_l}{\xi^r} = \sum_{k=0}^{Q} D_{kj}^r \phi_l(\xi_j)$$

where r is the order of differentiation and D is the Chebyshev spectral differentiation matrix. Substituting the above expressions in (24) - (27) yields.

$$\boldsymbol{H\,F\,l} = \boldsymbol{E} \quad (31)$$

Subject to

$$f_l(\xi_j) = 0;\ \sum_{k=0}^{Q} D_{0k}^r f_l(\xi_k) = 0;\ \theta_l(\xi_Q) = 0;\ \theta_l(\xi_0) = 0;\ \phi_l(\xi_Q) = 0;\ \phi_l(\xi_0) = 0 \quad (32)$$

Where $H = \begin{pmatrix} H_{1,1} & H_{1,2} & H_{1,3} \\ H_{2,1} & H_{2,2} & H_{2,3} \\ H_{3,1} & H_{3,2} & H_{3,3} \end{pmatrix}$

And

$$H_{1,1} = D^3 + a_1 + a_2 D^2 + a_3 D - (M + \lambda)D$$

$$H_{1,2} = GrI$$

$$H_{1,3} = GmI$$

$$H_{2,1} = b_1 P\,r\,I + b_3 P\,r\,\mathrm{D} - b_4 \mathrm{Pr} D$$

$$H_{2,2} = D^2 + b_2 PrD + \frac{1}{2}a_3 PrI - (M + \lambda)D$$

$$H_{2,3} = 0$$

$$H_{3,1} = c_1 ScI - c_3 ScD$$

$$H_{3,2} = -\tau c_3 ScD^2 - c_1 \tau ScD$$

$$H_{3,3} = D^2 + c_2 ScD - Scb_5 I - \tau Scb_1 D - a_4 ScI$$

$$F_l = \left[f_l(\xi_0), f_l(\xi_1), \dots, f_l(\xi_Q), \theta_l(\xi_0), \theta_l(\xi_1), \dots, \theta_l(\xi_Q), \phi_l(\xi_0), \phi_l(\xi_1), \dots, \phi_l(\xi_Q)\right]^T$$

$$E = \left[A_1(\xi_0), A_1(\xi_1), \dots, A_1(\xi_Q), A_2(\eta_0), A_2(\eta_1), \dots, A_2(\eta_Q), A_3(\eta_0), A_3(\eta_1), \dots, A_3(\eta_Q)\right]$$

$$a_1 = diag\left(\left[a_1(\eta_0), a_1(\eta_1), \dots, a_1(\eta_{Q-1}), a_1(\eta_Q)\right]\right)$$

$$b_1 = diag\left(\left[b_1(\eta_0), b_1(\eta_1), \dots, b_1(\eta_{Q-1}), b_1(\eta_Q)\right]\right)$$

$$c_1 = diag\left(\left[c_1(\eta_0), c_1(\eta_1), \dots, c_1(\eta_{Q-1}), c_1(\eta_Q)\right]\right)$$

i= 1, 2, 3, 4, 5.

In the above definitions, the superscript T denotes transpose, diag is a diagonal matrix and I is an identity matrix of size $(Q+1) \times (Q+1)$. To implement the boundary conditions (32), we delete the first and the last rows and columns of E and delete the first and last rows of functions $f_l(\xi), \theta_l(\xi), \phi_l(\xi)$ and E. The boundary conditions (32) are imposed on the resulting first and last rows of the modified matrix E and setting the resulting first and last rows of the modified matrix E to be zero.

The values of $f_l(\xi_0), f_l(\xi_1), \dots, f_l(\xi_Q), \theta_l(\xi_0), \theta_l(\xi_1), \dots, \theta_l(\xi_Q), \phi_l(\xi_0), \phi_l(\xi_1), \dots, \phi_l(\xi_Q)$ are then determined from

$$F_l = H^{-1}\boldsymbol{E} \tag{33}$$

To find the SHAM solutions of (16) - (18) we begin by defining the following linear operator:

$$L_f\left[\bar{f}(\eta; q), \bar{\theta}(\eta; q), \bar{\phi}(\eta; q)\right] = f''' + f f'' + a_1 f + a_2 f'' - (f')^2 + G r \theta + G m \phi - (M + \lambda) f' \tag{34}$$

$$L_\theta\left[\bar{f}(\eta; q), \bar{\theta}(\eta; q), \bar{\phi}(\eta; q)\right] = \theta'' + P r f \theta' + b_1 P r f + b_2 P r \theta' + P r E c (f'')^2 + b_3 P r E c f'' - Pr f'\theta - b_4 P r f' + \frac{1}{2} P r a_3 \theta \tag{35}$$

$$L_\phi\left[\bar{f}(\eta; q), \bar{\theta}(\eta; q), \bar{\phi}(\eta; q)\right] = \phi'' + Sc f \phi' + c_1 Sc f + c_2 Sc \phi' - Sc\tau\theta''\phi - Sc\tau c_3\theta'' - Sc\tau b_5\phi - Sc\tau\theta'\phi' - Sc\tau c_1\theta' - Sc\tau b_1\phi' - Sc f'\phi - c_3 Sc f' - a_4 Sc\phi \tag{36}$$

qϵ [0, 1] is an embedding parameter and $\bar{f}(\eta; q), \bar{\theta}(\eta; q), \bar{\phi}(\eta; q)$ are the unknown functions.

The zeroth order deformation is given as:

$$(1-q)L_f\left[\bar{f}(\eta; q) - \bar{f}_0(\eta),\right] = q\hbar_f K_{\bar{f}}(\eta) N_{\hbar_f}\left[\bar{f}(\eta; q), \bar{\theta}(\eta; q), \bar{\phi}(\eta; q)\right] \tag{37}$$

$$(1-q)L_\theta\left[\bar{f}(\eta; q) - \bar{f}_0(\eta),\right] = q\hbar_\theta K_{\bar{\theta}}(\eta) N_{\hbar_\theta}\left[\bar{f}(\eta; q), \bar{\theta}(\eta; q), \bar{\phi}(\eta; q)\right] \tag{38}$$

$$(1-q)L_\phi\left[\bar{f}(\eta; q) - \bar{f}_0(\eta),\right] = q\hbar_\phi K_{\bar{\phi}}(\eta) N_{\hbar_\phi}\left[\bar{f}(\eta; q), \bar{\theta}(\eta; q), \bar{\phi}(\eta; q)\right] \tag{39}$$

Where $\hbar_f, \hbar_\theta$ *and* $\hbar_\phi$ are the non-zero convergence controlling auxiliary parameters and $N_{\hbar_f}, N_{\hbar_\theta}$ *and* $N_{\hbar_\phi}$ are non- linear operators given by:

$$N_{\hbar_f}\left[\bar{f}(\eta; q), \bar{\theta}(\eta; q), \bar{\phi}(\eta; q)\right] = \bar{f}''' + \bar{f}\bar{f}'' + a_1\bar{f} + a_2\bar{f}'' - \left(\bar{f}'\right)^2 + G r \bar{\theta} + G m \bar{\phi} - (M + \lambda)\bar{f}' \tag{40}$$

$$N_{\hbar_\theta}\left[\bar{f}(\eta; q), \bar{\theta}(\eta; q), \bar{\phi}(\eta; q)\right] = \bar{\theta}'' + P r \bar{f}\bar{\theta}' + b_1 P r \bar{f} + b_2 P r \bar{\theta}' + P r E c \left(\bar{f}''\right)^2 + b_3 P r E c \bar{f}'' - Pr\bar{f}'\theta - b_4 P r \bar{f}' + \frac{1}{2} P r a_3 \bar{\theta} \tag{41}$$

$$N_{\hbar_\phi}\left[\bar{f}(\eta; q), \bar{\theta}(\eta; q), \bar{\phi}(\eta; q)\right] = \bar{\phi}'' + Sc\bar{f}\bar{\phi}' + c_1 Sc\bar{f} + c_2 Sc\phi' - Sc\tau\theta''\bar{\phi} - Sc\tau c_3\theta'' - Sc\tau b_5\bar{\phi} - Sc\tau\theta'\bar{\phi}' - Sc\tau c_1\theta' - Sc\tau b_1\bar{\phi}' - Sc\bar{f}'\bar{\phi} - c_3 Sc\bar{f}' - a_4 Sc\bar{\phi} \tag{42}$$

Differentiating (37) - (39) severally by m times with respect to q and then setting $q = 0$ and finally dividing the resulting equations by $m!$ yields the m th order deformation equations:

$$L_{\bar{f}}\left[\bar{f}(\varepsilon) - \chi_m \bar{f}_{m-1}(\varepsilon),\right] = \hbar_f K_{\bar{f}}(\varepsilon) R_m^{\bar{f}}(\varepsilon) \tag{43}$$

$$L_{\bar{\theta}}\left[\bar{\theta}(\varepsilon) - \chi_m \bar{\theta}_{m-1}(\varepsilon),\right] = \hbar_{\bar{\theta}} K_{\bar{\theta}}(\varepsilon) R_m^{\bar{\theta}}(\varepsilon) \tag{44}$$

$$L_{\bar{\phi}}[\bar{\phi}(\varepsilon) - \chi_{\mathrm{m}}\bar{\phi}_{\mathrm{m-1}}(\varepsilon),] = \hbar_{\bar{\phi}}K_{\bar{\phi}}(\varepsilon)R_m^{\bar{\phi}}(\varepsilon) \tag{45}$$

Subject to

$$\bar{f}_{\mathrm{m}}(-1) = 0; \bar{\theta}_{\mathrm{m}}(-1) = 0; \bar{\phi}_{\mathrm{m}}(-1) = 0; \bar{f}_{\mathrm{m}}(-1) = 0; \bar{\theta}_{\mathrm{m}}(-1) = 0; \bar{\phi}_{\mathrm{m}}(-1) = 0 \tag{46}$$

Where

$$R_m^{\bar{f}}(\varepsilon) = \bar{f}'''_{m-1} + \mathrm{a}_1\bar{f}_{\mathrm{m-1}} + \mathrm{a}_2\bar{f}''_{m-1} + \mathrm{a}_3\bar{f}'_{m-1} + G\,r\,\bar{\theta}_{\mathrm{m-1}} + G\,m\,\bar{\phi}_{\mathrm{m-1}} - (\mathrm{M}+\lambda)\bar{f}'_{m-1} + \sum_{n=0}^{m-1}\left[\bar{f}_{\mathrm{m-1}}\bar{f}''_{m-1-n} + (-1)f'_n f'_{m-1-n}\right] - A_1(\eta)(1-\chi_{\mathrm{m}}) \tag{47}$$

$$R_m^{\bar{\theta}}(\varepsilon) = \bar{\theta}''_{m-1} + \mathrm{b}_1 Pr\bar{f}_{\mathrm{m-1}} + \mathrm{b}_2 Pr\bar{\theta}'_{m-1} + \mathrm{b}_3 PrEc\bar{f}''_{m-1} - \mathrm{b}_4 Pr\bar{f}'_{m-1} + \frac{1}{2}Pr\mathrm{a}_3\bar{\theta}''_{m-1} + \sum_{n=0}^{m-1}\left[Pr\bar{f}_{\mathrm{n}}\bar{\theta}'_{m-1-n} + PrEc\bar{f}''_n\bar{f}''_{m-1-n} - Pr\bar{f}'_{m-1}\bar{\theta}''_{m-1-n}\right] - A_2(\eta)(1-\chi_{\mathrm{m}}) \tag{48}$$

$$R_m^{\bar{\phi}}(\varepsilon) = \bar{\phi}''_{m-1} + \mathrm{c}_1 Sc\bar{f}_{\mathrm{m-1}} + \mathrm{c}_2 Sc\bar{\phi}'_{m-1} + \mathrm{c}_3 Sc\tau\bar{\theta}''_{m-1} - \mathrm{b}_5 Sc\tau\phi_{\mathrm{m-1}} - \mathrm{c}_1 Sc\tau\bar{\theta}'_{m-1} - \mathrm{c}_3 Sc\bar{f}'_{m-1} - \mathrm{a}_4 Sc\bar{\phi}'_{m-1} + \sum_{n=0}^{m-1}\left[Sc\bar{f}_{\mathrm{n}}\bar{\theta}'_{m-1-n} - \tau Sc\bar{\theta}''_n\bar{\phi}'_{m-1-n} - Sc\bar{f}_{\mathrm{n}}\bar{\phi}_{\mathrm{m-1}}\right] - A_3(\eta)(1-\chi_{\mathrm{m}}) \tag{49}$$

And

$$\chi_{\mathrm{m}} = \begin{cases} 0 \; when \; m \leq 1 \\ 1 \; when \; m > 1 \end{cases} \tag{50}$$

Applying the Chebyshev pseudospectral transformation on (43) - (45) gives

$$\mathbf{H}\,\bar{f}_{\mathrm{m}} = \left(\chi_{\mathrm{m}} + \hbar_f\right)\mathbf{H}\,\bar{f}_{\mathrm{m-1}} - \hbar_f(1-\chi_{\mathrm{m}})E + \hbar_f Z_{m-1}^{\bar{f}} \tag{51}$$

$$\mathbf{H}\,\bar{\theta}_{\mathrm{m}} = (\chi_{\mathrm{m}} + \hbar_\theta)\,\mathbf{H}\,\bar{\theta}_{\mathrm{m-1}} - \hbar_\theta(1-\chi_{\mathrm{m}})E + \hbar_\theta Z_{m-1}^{\bar{\theta}} \tag{52}$$

$$\mathbf{H}\,\bar{\phi}_{\mathrm{m}} = \left(\chi_{\mathrm{m}} + \hbar_\phi\right)\mathbf{H}\,\bar{\phi}_{\mathrm{m-1}} - \hbar_\phi(1-\chi_{\mathrm{m}})E + \hbar_\phi Z_{m-1}^{\bar{\phi}} \tag{53}$$

Subject to

$$\bar{f}_{\mathrm{m}}(\varepsilon_Q) = 0; \sum_{n=0}^{m-1} D_{0\mathrm{k}}\bar{f}_{\mathrm{m}}(\varepsilon_k) = 0; \bar{\theta}_{\mathrm{m}}(\varepsilon_Q) = 0; \bar{\theta}_{\mathrm{m}}(\varepsilon_0) = 0; \bar{\phi}_{\mathrm{m}}(\varepsilon_Q) = 0; \bar{\phi}_{\mathrm{m}}(\varepsilon_0) = 0 \tag{54}$$

Where **H** and **E** are as defined above and

$$F_{\mathrm{m}} = \left[\bar{f}_{\mathrm{m}}(\varepsilon_0), \bar{f}_{\mathrm{m}}(\varepsilon_1), \ldots, \bar{f}_{\mathrm{m}}(\varepsilon_Q), \bar{\theta}_{\mathrm{m}}(\varepsilon_0), \bar{\theta}_{\mathrm{m}}(\varepsilon_1), \ldots, \bar{\theta}_{\mathrm{m}}(\varepsilon_Q), \bar{\phi}_{\mathrm{m}}(\varepsilon_0), \bar{\phi}_{\mathrm{m}}(\varepsilon_1), \ldots, \bar{\phi}_{\mathrm{m}}(\varepsilon_Q)\right]^T$$

$$Z_{m-1}^{\bar{f}} = \sum_{n=0}^{m-1}\left[\left(\bar{f}_{\mathrm{n}}\right)(\mathrm{D}^2)\bar{f}_{\mathrm{m-1-n}} + (-1)(D\bar{f}_{\mathrm{n}})(D\bar{f}_{\mathrm{m-1-n}})\right] \tag{55}$$

$$Z_{m-1}^{\bar{\theta}} = \sum_{n=0}^{m-1}\left[Pr\left(\bar{f}_{\mathrm{n}}\right)(\mathrm{D}\bar{\theta}_{\mathrm{m-1-n}}) + PrEc\left(\mathrm{D}^2\bar{f}_{\mathrm{n}}\right)\left(\mathrm{D}^2\bar{f}_{\mathrm{m-1-n}}\right) - Pr\left(D\bar{f}_{\mathrm{n}}\right)\left(\bar{\theta}_{\mathrm{m-1-n_n}}\right)\right] \tag{56}$$

$$Z_{m-1}^{\bar{\phi}} = \sum_{n=0}^{m-1}\left[Sc\left(\bar{f}_{\mathrm{n}}\right)(\mathrm{D}\bar{\phi}_{\mathrm{m-1-n}}) - \tau Sc(\mathrm{D}^2\bar{\theta}_{\mathrm{n}})(\mathrm{D}\bar{\phi}_{\mathrm{m-1-n}}) - \tau Sc(\mathrm{D}\bar{\theta}_{\mathrm{n}})(\mathrm{D}\bar{\phi}_{\mathrm{m-1-n}}) - Sc\left(D\bar{f}_{\mathrm{n}}\right)(\bar{\phi}_{\mathrm{m-1-n}})\right] \tag{57}$$

To implement the boundary conditions above we delete the first and last rows of $Z_{m-1}^{\bar{f}}, Z_{m-1}^{\bar{\theta}}, Z_{m-1}^{\bar{\phi}}$ and E and delete the first and last rows and first and last columns of H in (51 − 53). The boundary conditions (54) are imposed on the first and last row of the modified H matrix on the left side of the equal sign in (51 − 53). The first and last rows of the modified H matrix on the right of the equal sign in (51 − 53) are the set to be zero. This results in the following recursive formulas:

$$\bar{f}_{\mathrm{m}} = \left(\chi_{\mathrm{m}} + \hbar_f\right)\mathrm{H}^{-1}\,\mathrm{H}\bar{f}_{\mathrm{m-1}} + \hbar_f\mathrm{H}^{-1}\left[\hbar_f Z_{m-1}^{\bar{f}} - (1-\chi_{\mathrm{m}})E\right] \tag{58}$$

$$\bar{\theta}_{\mathrm{m}} = (\chi_{\mathrm{m}} + \hbar_\theta)\mathrm{H}^{-1}\mathrm{H}\bar{\theta}_{\mathrm{m-1}} + \hbar_\theta\mathrm{H}^{-1}\left[\hbar_\theta Z_{m-1}^{\bar{\theta}} - (1-\chi_{\mathrm{m}})E\right] \tag{59}$$

$$\bar{\phi}_{\mathrm{m}} = \left(\chi_{\mathrm{m}} + \hbar_\phi\right)\mathrm{H}^{-1}\mathrm{H}\bar{\phi}_{\mathrm{m-1}} + \hbar_\phi\mathrm{H}^{-1}\left[\hbar_\phi Z_{m-1}^{\bar{\phi}} - (1-\chi_{\mathrm{m}})E\right] \tag{60}$$

Thus, starting from the initial approximation, obtain from (33), higher-order approximations $\bar{f}_{\mathrm{m}}(\varepsilon), \bar{\theta}_{\mathrm{m}}(\varepsilon), \bar{\phi}_{\mathrm{m}}(\varepsilon)$ for $\mathrm{m} \geq 1$ can be obtained through the recursive formula (58) - (60).

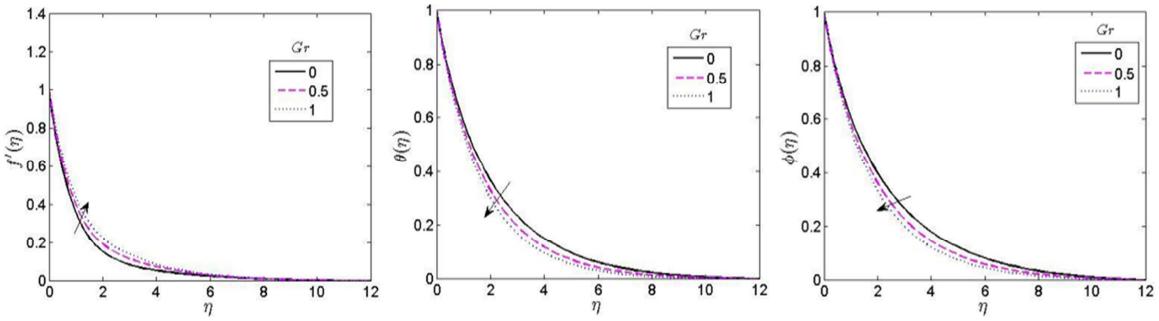

Figure 2. *Velocity, Temperature and Concentration profiles for different values of thermal grashof number (Gr).*

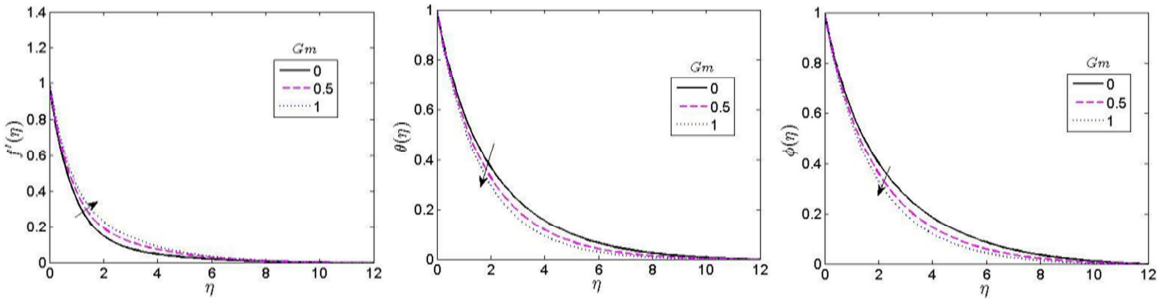

Figure 3. *Velocity, Temperature and Concentration profiles for different values of concentration grashof number (Gm).*

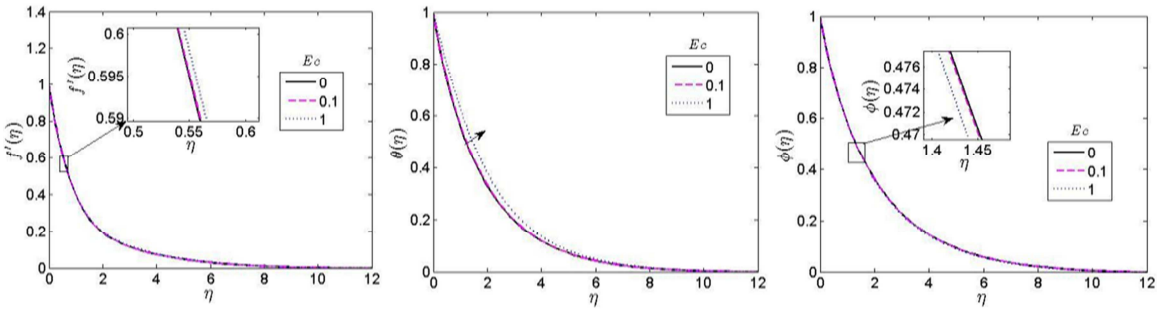

Figure 4. *Velocity, Temperature and Concentration profiles for different values of Eckert number (Ec).*

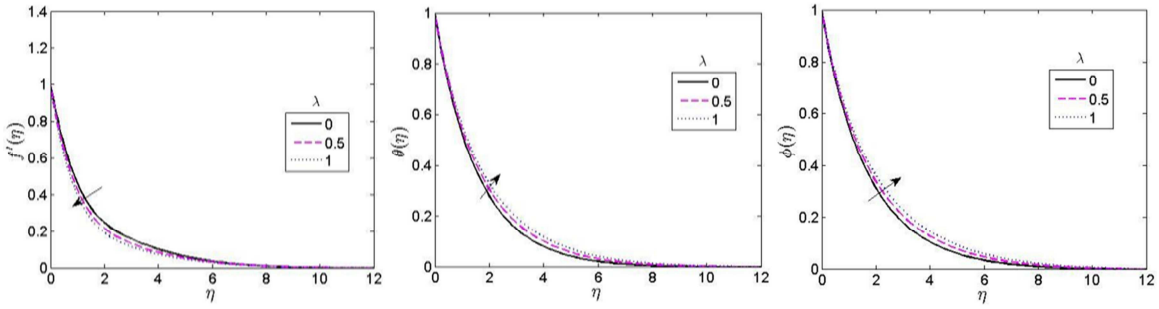

Figure 5. *Velocity, Temperature and Concentration profiles for different values of porosity parameter (λ).*

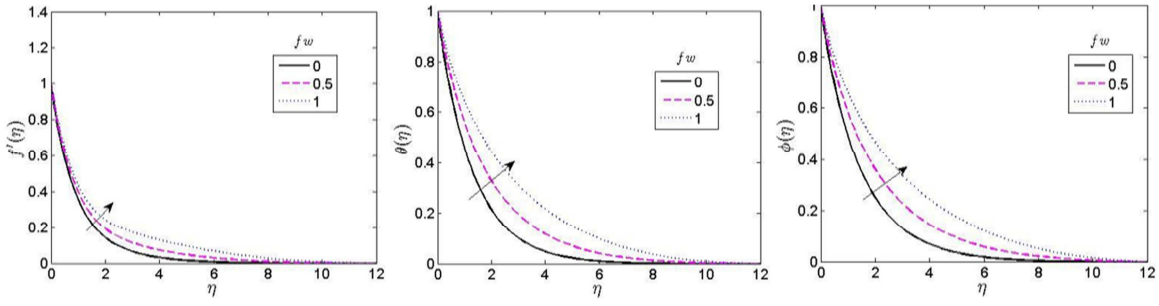

Figure 6. *Velocity, Temperature and Concentration profiles for different values of suction/injection parameter (fw).*

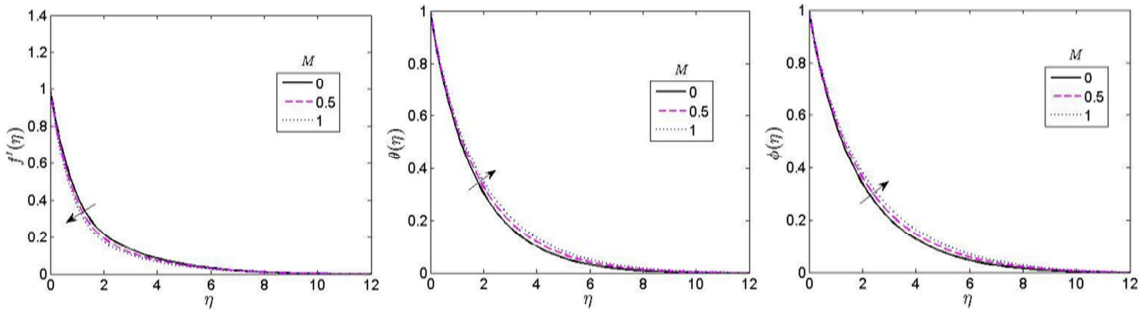

Figure 7. *Velocity, Temperature and Concentration profiles for different values of Magnetic parameter (M).*

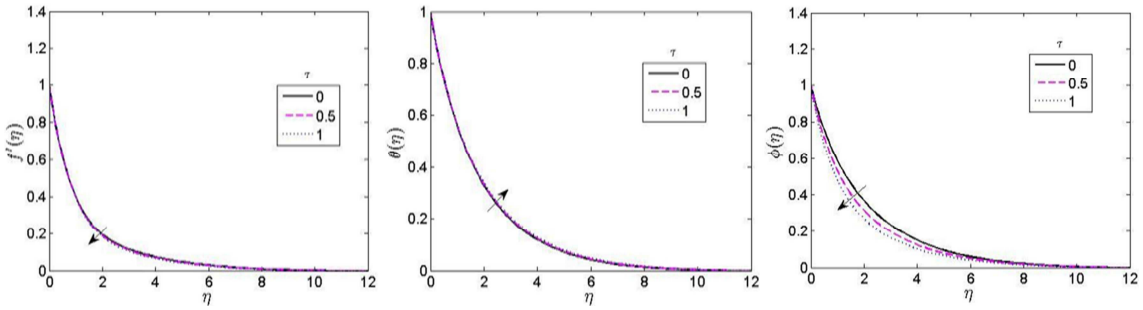

Figure 8. *Velocity, Temperature and Concentration profiles for different values of thermophoretic parameter (τ).*

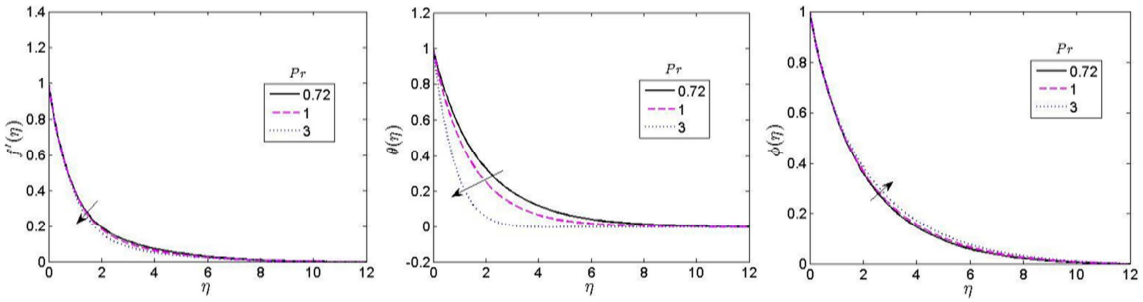

Figure 9. *Velocity, Temperature and Concentration profiles for different values of Prandtl number (Pr).*

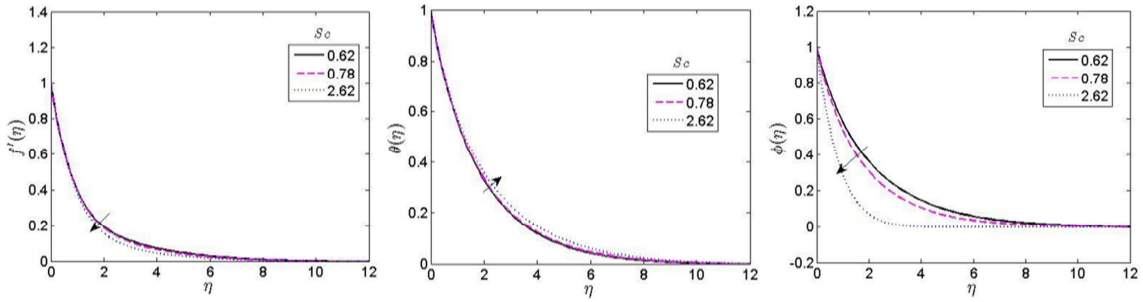

Figure 10. *Velocity, Temperature and Concentration profiles for different values of Schmidt number (Sc).*

Table 1. *Comaprison results for $f''(0)$, $\theta'(0)$, $\phi'(0)$ at various values of suction parameter f_w and Grashof number (Buoyancy force) when P r =0.72, Gc = M = 0.1, Sc = 0.62, τ = Ec = λ = 0.*

f_w	Gr	Ibrahim and Makinde [28]			Gangadhar and Bhaskar [29]			Present Results (SHAM)		
		f''(0)	$\theta'(0)$	$\phi'(0)$	f''(0)	$\theta'(0)$	$\phi'(0)$	f''(0)	$\theta'(0)$	$\phi'(0)$
0	0.1	0.888971	0.7965511	0.7253292	0.897945	0.805082	0.740192	0.89766087	0.8052544	0.73938283
	0.5	0.695974	0.8379008	0.7658018	0.70684	0.841012	0.773803	0.7065596	0.841176	0.79254957
	1.0	0.475058	0.8752835	0.8020042	0.485886	0.876165	0.806773	0.48560737	0.87630582	0.80506679
1	0.1	0.570663	0.601256	0.5271504	0.575823	0.566525	0.537923	0.57573573	0.56656241	0.53139812
	0.5							0.40975174	0.59744769	0.56027165
	1.0							0.21449625	0.62828717	0.58916319
3	0.1	0.275153	0.2955702	0.2902427	0.0030192	0.143197	0.143829	0.27532986	0.29636384	0.29000008
	0.5							0.16674285	0.30784998	0.30142208
	1.0							0.03336961	0.32101847	.031455527

Table 2. *Comaprison of computational results for local skin friction $f''(0)$, local nusselt number $-\theta'(0)$, and the local sherwood number $-\phi'(0)$ at various values of Parameter parameter λ at Pr = 0.72, Gr = Gm = M = f_w = 0.1, Sc = 0.62, τ = Ec = 0.*

	Gangadhar and Bhaskar [29]			**Present Results (SHAM)**		
	f''(0)	**$-\theta'(0)$**	**$-\phi'(0)$**	**f''(0)**	**$-\theta'(0)$**	**$-\phi'(0)$**
0.1	0.94458	0.795952	0.531689	0.94433684	0.79611208	0.73096907
0.5	1.11654	0.762949	0.701131	1.11634577	0.76306844	0.70069542
1.0	1.30551	0.728382	0.669421	1.30541709	0.72846466	0.66922502
1.5	1.47358	0.699551	0.643201	1.47352151	0.69961016	0.64315628
2.0	1.62614	0.675081	0.621099	1.62606555	0.67512251	0.62115071
3.0	1.89742	0.635561	0.585681	1.89741014	0.63558577	0.58583287

Table 3. *SHAM computational results for local skin friction $f''(0)$, local nusselt number $-\theta'(0)$, and the local sherwood number $-\phi'(0)$ at various values of viscous dissipation parameter Ec at Pr = 0.72, Gr = Gm = M = f_w = 0.5, λ = 1.0, Sc = 0.62, τ = 0.05.*

Ec	**f'**	**$-\theta'$**	**$-\phi'$**
0	0.96530733	0.61596720	0.57744647
0.5	0.96523728	0.61364809	0.57741284
1	0.97425255	0.60877466	0.82904155

Table 4. *SHAM computational results for local skin friction $f''(0)$, local nusselt number $-\theta'(0)$, and the local sherwood number $-\phi'(0)$ at various values of thermophoretic force τ at Pr = 0.72, Gr = Gm = M = f_w = 0.5, λ = 1.0, Sc = 0.62, Ec = 0.01.*

τ	**f'**	**$-\theta'$**	**$-\phi'$**
0	0.96472892	0.61394434	0.56472546
0.5	0.96965777	0.61116921	0.69417842
1	0.97425255	0.60877466	0.82904155

4. The Findings and Discussion

Numerical calculation using the spectral homotopy analysis approach has been done in order to examine the model to better understand the impact of viscous dissipation and thermophoresis, and the findings have been provided in the form of graphs and tables.

Different flow parameters, including the Eckert number (Ec), magnetic parameter (M), Prandtl number (Pr), thermophoretic parameter (τ), porosity parameter (λ), thermal Grashof number (Gr), concentration Grashof number (Gm), and suction/injection parameter, have all been computed numerically using SHAM.

The following default parametric parameters are used for the sham computations in order to discuss our results:

Ec = 0.01, Gr = Gm = M = = 0.5, Pr = 0.72, Sc = 0.62, λ = 1.0, τ =0.05 to gain a thorough understanding of the issue's mechanics. Therefore, unless otherwise noted, all graphs correspond to these values. Additionally, the boundary condition (η_{max}= 12) is close enough to the actual stream velocity to allow the flow profiles to approach it. The prandtl number (Pr = 0.72) was chosen to represent air, and the values of the Schmidt numbers (Sc = 0.62, 0.78, and 2.62) were selected to represent the dispersing chemical species of most common interest in air, such as O and Propyl Benzene. The results of this work are a more extended version of those found in Ibrahim and Makinde [28] and Gangadhar and Bhaskar [29] in the absence of the viscosity parameter (Ec), thermophoresis force (τ), and permeability parameter (λ).

The SHAM results as presented in Tables 1 and 2 are in great agreement with the results reported in the literature, for example, when (Ec = 0). The values of skin-friction coefficient, local heat transfer rate, and sherwood number have been determined for various values of the permeability parameter (λ), viscous dissipation Ec, and thermophoretic parameter (τ) in order to assess the correctness of the current solution technique (SHAM) (see Tables 2-4). The impact of the permeability parameter (λ) on the flow profiles is seen in Table 2. The generation of the skin friction coefficient and sherwood number are both enhanced by an increase in the permeability parameter on the flow regime, whilst the rate of local heat transfer is decreased. Surprisingly, the results of the model analysis by Gangadhar and Bhaskar [29] and those obtained using the spectral homotopy analysis method agreed. Table 3 shows that flow physical quantities like skin friction coefficient, nusselt number, and sherwood number significantly decrease as viscous dissipation parameter (Ec) varies from 0 to 1.0. This further supported the idea that, due to the link between the energy and momentum equations, viscous heating plays a significant role in the dynamics of fluids with significantly temperature-dependent viscosities. Table 4 shows that while the rate of local heat transfer is noticeably reduced, an increase in thermophoretic force facilitates the formation of momentum and concentration boundary layers due to an increase in skin-friction coefficient and sherwood number.

The graphic effects of the thermal grashof number Gr and the concentration grashof number Gm on the dimensionless velocity, temperature, and concentration profiles are shown in Figures 2 and 3, respectively. In our calculations, we took into account a scenario in which the buoyancy forces are assisting the flow, i.e., when the local temperature Grashof number (Gr > 0) and local concentration Grashof number (Gm > 0) are greater than zero (which indicates that the chemical species concentration in the free stream region is less than the concentration at the boundary surface). The flow's velocity profile rises with an increase in bouyancy

force Gr, Gm, but the temperature and concentration profiles fall. Figure 4 shows how the viscous dissipation term Eckert number Ec affects the dimensionless velocity, temperature, and concentration profiles of the flow. The flow's temperature and velocity profiles increase with an increase in Eckert number, but the fluid's concentration profile decreases. These figures show that Ec have very different effects on velocity and the thickness of the associated thermal boundary layer. This means that as the viscous dissipation term increases, so do the flow's velocity and temperature profile. This confirms that the Eckert number (Ec), when present, improves temperature distribution in a free convective flow. Figure 5 illustrates the effects of the permeability parameter on the flow profiles. It has been found that an increase in flow permeability causes the flow profile's temperature and concentration to rise while the velocity of the profile decreases.

The potential impact of the suction/injection parameter on the flow regime is shown in Figure 6. All of the profiles are seen to increase as the suction parameter increases. However, the impacts on velocity are minimal compared to those on temperature and concentration profiles. The impact of magnetic parameters on the flow profiles is depicted in Figure 7. The temperature and concentration flow profiles also increase in response to an increase in the magnetic parameter, whereas the velocity flow profile decreases. This is because a change in (M) causes a change in the magnetic field's Lorentz force, and the Lorentz force increases the resistance of the transport phenomenon. As a result, the boundary layer separates early and the momentum boundary layer thickness increases. Figure 7 shows that as the magnetic field strength increases, the fluid temperature rises. In other words, increasing (M) indicates that the magnetic field had an impact on the flow system by raising the temperature values in the flow field, lowering the gradient at the wall, and raising the thickness of the thermal boundary layer. While the magnetic parameter (M) increases along with the flow's concentration profile.

In the presence of the viscous dissipation term, Figure 8 illustrates the effect of the thermophoresis parameter (τ) on the dimensionless velocity, dimensionless temperature, and concentration. The velocity and concentration profiles in Figure 8 drop as the thermophoresis parameter increases due to viscous dissipation, which functions as a source of internal heat to the flow system. Along with it, fluid temperature profiles noticeably rise (see Figure 8). The impact of the thermophoretic parameter on the concentration profile is seen in Figure 8(c). As the thermophoretic parameter (τ) increases, it can be seen that the fluid concentration drops. Therefore, thermophoretic factors considerably change the concentration boundary layer.

The effect of the Prandtl number Pr on the flow system is depicted in Figure 9. Temperature and velocity profiles drastically drop as (Pr) grows in magnitude. An increase in the Prandtl number (Pr) at a certain value of specific heat capacity (c_p), and thermal conductivity ($\propto$) only denotes an increase in the degree of fluid viscosity. A low velocity profile is consistent with a high fluid viscosity value. It has been found that an increase in the Prandtl number causes temperature and the thickness of the thermal boundary layer to decrease, as well as the average temperature within the boundary layer to generally decrease. The reason is that heat can dissipate from the heated plate more quickly for lower values of (Pr) than at higher values, which is analogous to rising thermal conductivities. While Prandtl grows, the concentration profile does not. Schmidt number has a significant impact on the flow system's velocity, temperature, and concentration profiles, as shown in Figure 10. The flow velocity and concentration profiles both significantly drop when the Schmidt number rises from 0.62 to 2.62. While Schmidt number has the opposite impact on the flow's temperature.

5. Conclusion

The effect of thermophoresis and viscous dissipation on free convection boundary layer flow over a porous medium has been examined in this paper. The similarity transformations have been used to convert the governing equations and their related boundary conditions into dimensionless equations, and the resulting equations are then solved using the Spectral Homotopy Analysis Method (SHAM). When the computational results from SHAM are compared to those from the literature, they show a good degree of agreement. Our simulations demonstrate that the SHAM solution series converges to the numerical solution with an accuracy of up to six decimal places. In comparison to the traditional HAM and other numerical approaches mentioned in the reviewed literature, the SHAM appears to be more efficient because it provides greater freedom in selecting linear operators. The considerable impact of the flow parameters on the flow profiles has been expressively examined. Important findings include:

With an increase in the Magnetic field parameter and Permeability parameter, the Skin friction coefficient, Nusselt number, and Sherwood number decrease. The fluid's motion is slowed down by the magnetic field, which has a substantial impact on the velocity field.

With an increase in Grashof number or modified Grashof number, the velocity profiles rise.

The concentration profiles are significantly influenced by thermophoretic number. When compared to the sherwood number, the influence of the thermophoresis parameter on the local heat transfer rate is relatively considerable.

With an increase in Eckert number Ec, a term that describes viscous dissipation, the fluid velocity and temperature rise, while the concentration profile decreases.

Science and technology applications heavily rely on the analysis of the current investigation. The solutions to the current issue are particularly interesting for the production of polymers, glass or ceramics manufacturing, food processing, particle deposition onto wafers in the microelectronics industry, magnetically controlled metal welding or coating, polymer engineering, metallurgy, etc.

Nomenclature

U(x) - velocity of the flow
T∞ - free stream temperature of the surrounding fluid
u, v - velocity components in x- and y- respectively
g - gravitational force due to acceleration
Dm - coefficient of mass diffusivity
Cp - the specific heat at constant pressure
M - Magnetic parameter
Pr - Prandtl number
Gr - Thermal Grashof number
Gm - Concentration Grashof number
Sc - Schmidt number
K - real constant
B - real constant
a - real constant
b - real constant
Cf - Skin-friction coefficient
f - Dimensionless stream function
Nu - Nusselt number
Sh - Sherwood number
fw -suction/injection parameter
C∞ - free stream concentration
T - fluid temperature
Tw - wall temperature
C - fluid concentration
Cw - wall concentration
C - fluid concentration
Tref - reference temperature
Greek Symbols
μ - dynamic viscosity
λ - permeability parameter
ρ - density
βT - volumetric coefficient of thermal expansion
βc - volumetric coefficient of expansion
ν - kinematic viscosity
ϕ - dimensionless concentration
η - similarity variable
ψ - stream function
θ - dimensionless temperature
τ - Thermophoretic parameter

References

[1] S. L. Goren: Thermophoresis of Aerosol Particles in the Laminar Boundary Layer on a Flat Plate. J. Colloid Interface Sci. Vol. (61), 77-85, (1977).

[2] B. Chandra and M. Kumar: The Combined Effect of Chemical Reaction, Radiation on Heat and Mass Transfer along a Continuously Moving Surface in Presence of Thermophoresis. Journal of Applied Fluid Mechanics Vol. (6) 3, 351-356, (2013).

[3] M. S. Alam, M. M. Rahman and M. A. Sattar: Transient Magnetohydrodynamic Free Convective Heat and Mass Transfer Flow with Thermophoresis past a Radiate Inclined Permeable Plate in the Presence of Variable Chemical Reaction and Temperature Dependent Viscosity Nonlinear Analysis: Modelling and Control Vol. (14) 1, 3-20, (2009).

[4] U. N. Das, R. K. Deka and V. M. Soundalgekar: Effects of Mass Transfer on Flow Past an Impulsively started Infinite Vertical Plate with Constant Heat Flux and Chemical reaction. Forschung in Inge-Engg Research Vol. (60), 284-287, (1994).

[5] S. P. Anjali devi and R. Kandasamy: Effects of a chemical reaction heat and mass transfer on MHD flow past a semi-infinite plate. Z. Angew. Math. Mech. Vol. (80), 697-701, (2000).

[6] R. Kandasamy, K. Periasamy and K. K. S. Prabhu: Chemical reaction, heat and mass transfer on MHD flow over a vertical stretching surface with heat source and thermal stratification effects. International Journal Heat and Mass Transfer Vol. (48) 21-22, 4557- 4561, (2005).

[7] M. Q. Al-Odat and Al-Azab: Influence of chemical reaction on transient MHD free convection over a moving vertical plate. Emirates Journal of Engineering Research Vol. (12) 3, 15-21, (2007).

[8] S. Ahmed: Influence of chemical reaction on transient MHD free Convective flow over a vertical plate in slipflow Regime. Emirates Journal for Engineering Research Vol. (15) 1, 25-34, (2010).

[9] R. N. Jat and S. Chaudhary: Hydromagnetic Flow and heat transfer on a continuously moving surface. Applied Mathematical Sciences Vol. (4) 2, 65-78, (2010).

[10] B. Gebhart B: Effects of viscous dissipation in natural convection. Journal of Fluid Mechanics Vol. (14), 225- 232, (1962).

[11] H. G. Takhar and O. A. Beg: Effects of transverse magnetic field, Prandtl number and Reynolds number on non-Darcy mixed convective flow of an incompressible viscous fluid past a porous vertical flat plate in a saturated porous medium. International Journal of Energy Research. Vol. (21), 87-100, (1997).

[12] P. V. S. N. Murthy and P. Singh: Effect of viscous dissipation on a non-Darcy natural convection regime. International Journal of Heat and Mass Transfer Vol. (40), 1251-1260, (1997).

[13] D. A. S. Rees, E. Magyari, and B. Keller: The development of the asymptotic viscous dissipation profile in a vertical free convective boundary layer flow in a porous medium. Transport in Porous Media Vol (53), 347-355, (2003).

[14] D. A. Nield: The modeling of viscous dissipation in a saturated porous medium. Journal of Heat Transfer Vol. (129) 1459, (2007).

[15] P. Loganathan, Arasu P. Puvi: Thermophoresis effects on non-darcy mhd mixed convective heat and mass transfer past a porous wedge in the presence of suction/ injection. Theoret. Appl. Mech., 37 (3), 203-227, (2010).

[16] A. Mahdy: Thermophoresis particle deposition and variable viscosity effects on non-darcy free convection in a fluid saturated porous media with uniform suction/injection. Latin America Applied Research Vol. (43), 113-119, (2013).

[17] Felix Ilesanmi Alao, Chika Uchechukwu Boneze, Adeyemi Isaiah Fagbade. Soret and Dufour Effects on Heat and Mass Transfer of Boundary Layer Flow over Porous Wedge with Thermal Radiation: Bivariate Spectral Relaxation Method. American Journal of Chemical Engineering. Vol. 7, No. 1, 2019, pp. 7-21. doi: 10.11648/j.ajche.20190701.12.

[18] Muhaimin I., Kandasamy R. and Kamis A. B.: Thermophoresis and chemical reaction effects on MHD mixed convective heat and mass transfer past a porous wedge in the presence of suction. Latin America Applied Research 40 (2), ISSN 1851-8796, (2008).

[19] N. Kishan and S. Maripala: Thermophoresis and viscous dissipation effects on darcy-forcheimer MHD mixed convection in a fluid saturated porous media. Advances in Applied Science Research Vol. (3), 60-74, (2012).

[20] A. I. Fagbade, B. O Falodun and C. U. Boneze: The influence of magnetic field, viscous dissipation, and thermophoresis on darcy-forcheimer mixed convection flow in fluid saturated porous media. American Journal of Computational Mathematics Vol. (5), 18-40. http://dx.doi.org/10.4236/ajcm.2015.51002, (2015).

[21] Talbot, L., Cheng, R. K., Scheffer, R. W. and Wills, D. R.: Thermophoresis of Particles in a Heated Boundary Layer. Journal of Fluid Mechanics Vol. (101), 737-758, (1980). http://dx.doi.org/10.1017/S0022112080001905.

[22] Canuto, C., Hussaini, M. Y., Quarteroni, A. and Zang, T. A.: Spectral Methods in Fluid Dynamics. SpringerVerlag, Berlin, (1988). http://dx.doi.org/10.1007/978-3-642-84108-8.

[23] Trefethen, L. N.: Spectral Methods in MATLAB. SIAM, Philadelphia, (2000), http://dx.doi.org/10.1137/1.9780898719598.

[24] Liao, S. J.: Beyond Perturbation: Introduction to the Homotopy Analysis Method. Chapman and Hall/CRC Press, Boca Raton, (2003). http://dx.doi.org/10.1201/9780203491164.

[25] Liao, S. J.: Homotopy Analysis Method in Nonlinear Differential Equations. Springer and Higher Education Press, Berlin Beijing, (2012). http://dx.doi.org/10.1007/978-3-642-25132-0.

[26] Motsa, S. S., Sibanda, P. and Shateyi, S.: A New Spectral-Homotopy Analysis Method for Solving a Nonlinear Second Order BVP. Communications in Nonlinear Science and Numerical Simulation, Vol. (15), 2293-2302, (2010). http://dx.doi.org/10.1016/j.cnsns.2009.09.019.

[27] Motsa, S. S., Sibanda, P., Awad, F. G. and Shateyi, S. A New Spectral-Homotopy Analysis Method for the MHD Jeffery-Hamel Problem. Computers and Fluids Vol. (39), 1219-1225, (2010).

[28] S. Y. Ibrahim and O. D. Makinde: Chemically reacting MHD boundary layer flow of heat and mass transfer over a moving vertical plate with suction. Scientific Research and Essays, 5 (19), 2875-2882, (2010).

[29] K. Gangadhar and N. Bhaskar Reddy: Chemically Reacting MHD Boundary Layer Flow of Heat and Mass Transfer over a Moving Vertical Plate in a Porous Medium with Suction. Journal of Applied Fluid Mechanics, Vol. 6, No. 1, pp. 107-114, (2013).